symmetry

MDPI

Article

Stability Analysis of the Solution for the Mixed Integral Equation with Symmetric Kernel in Position and Time with Its Applications

Faizah M. Alharbi

Mathematics Department, Faculty of Sciences, Umm Al-Quraa University, Makkah 24227, Saudi Arabia; fmharbi@uqu.edu.sa

Abstract: Under certain assumptions, the existence of a unique solution of mixed integral equation (MIE) of the second type with a symmetric kernel is discussed, in $L_2[\Omega] \times C[0,T], T < 1$, Ω is the position domain of integration and T is the time. The convergence error and the stability error are considered. Then, after using the separation technique, the MIE transforms into a system of Hammerstein integral equations (SHIEs) with time-varying coefficients. The nonlinear algebraic system (NAS) is obtained after using the degenerate method. New and special cases are derived from this work. Moreover, numerical results are computed using MATLAB R2023a software.

Keywords: continuous and symmetric kernel; integral equation of Volterra–Hammerstein; degenerate method; system of Hammerstein; numerical results

Citation: Alharbi, F.M. Stability Analysis of the Solution for the Mixed Integral Equation with Symmetric Kernel in Position and Time with Its Applications. *Symmetry* **2024**, *16*, 1048. https://doi.org/10.3390/sym16081048

Academic Editor: Omar Bazighifan

Received: 16 July 2024
Revised: 8 August 2024
Accepted: 10 August 2024
Published: 14 August 2024

1. Introduction

It is known that integral equations are the structural origin of differential equations. Therefore, it is natural and known that to solve a differential equation or transform it into an integral equation, the solution outcome depends on the given conditions. If the given conditions are initial, the result represents the Volterra integral equation. If the conditions are marginal, the result represents the Fredholm integral equation. If the conditions are mixed, we obtain the Volterra–Fredholm integral equation. We find these types of problems frequently in contact problems in elasticity science or mixed problems in communication mechanics and other applied sciences.

The versatility of integral equations (IEs), with their various forms, permits the simulation of a broad array of issues in the realm of fundamental sciences, prompting a considerable effort by researchers to present the solutions to these systems. Scientists have used many different ways to solve these problems, which shows that they are getting better quickly.

The orthogonal polynomial approach is well recognized as a crucial tool for solving diverse scientific challenges encountered in numerous fields of study. Alhazmi [1] employed a novel method to extract several spectral connections from the mixed integral equation. He did this by combining the generalized potential kernel with variable separation and orthogonal polynomials. Nemati et al.'s study [2] used a novel method that included a continuous kernel to examine the output of the two-dimensional (2D) Volterra integral model. Hafez and Youssri [3] examined the numerical solutions of the two-dimensional integral model, which is founded on the linear Volterra–Fredholm equation. They employed the collocation method using the Legendre–Chebyshev polynomials. In their study, Abdou et al. [4] employed Chebyshev polynomials to effectively address quadratic integral equations that incorporate a phase-lag factor in the time domain.

Presently, numerous studies have focused on developing advanced and efficient methods for solving the integral equations (IEs) and integral differential equations (Io-DEs). These include the utilization of Riemann–Stieltjes integral conditions [5,6], the application

of the Lerch polynomial method [7,8], and the implementation of the Spectral Legendre–Chebyshev method [9]. Additionally, numerical observations based on semi-analytical approaches in [10] have been employed to solve the VIEs. The wavelet collocation method was used [11] for solving fractional integro-differential equations (FrIo-DEs). In [12], the authors applied the extended cubic B-spline to interpret the collocation strategy to solve the FrIo-DEs. Zhang and Li, in [13], establish the basic structure of the exponential Euler difference form for Caputo–Fabrizio fractional-order differential equations with multiple lags. This kind of study provides a deep understanding of behavior for modifying systems.

The linear and nonlinear integral equations (LIEs/NIEs) are utilized in airfoil analysis, quantum mechanics, astrophysics, and lasers; see [14–20].

Consider the NIE of the second kind of type Volterra–Hammerstein in $(n+1)$ dimensional

$$\begin{gathered}\mu U(u,t) = H(u,t) + \lambda \int_0^t \int_\Omega f(t,\tau) p(u,y) Z(\tau,w,U(w,\tau)) dw d\tau, (\mu, \lambda - constants) \\ (u = \overline{u}(u_1,u_2,...,u_n), w = \overline{w}(w_1,w_2,...,w_n))\end{gathered} \tag{1}$$

Here, in Equation (1), the given functions $H(u,t), Z(t,u,U(u,t))$ belong to $L_2(\Omega) \times C[0,T]$—space. The integration domain Ω is a closed bounded set and depends on the vector of position, while the time $t \in [0,T]$. The kernel $p(u,w) \in L_2([\Omega] \times [\Omega])$, while $f(t,\tau) \in C([0,T] \times [0,T]); t, \tau \in [0,T], T < 1$. The constant μ describes the type of the integral equation, and λ carries a physical significance. Finally, $U(u,t)$ is the unknown function and will be discussed in the space of the given function $H(u,t)$.

Differentiating Equation (1) with respect to the variable t, we obtain

$$\begin{gathered}\mu \frac{\partial U(u,t)}{\partial t} = \frac{\partial H(u,t)}{\partial t} + \lambda f(t,t) \int_\Omega p(u,w) Z(t,w,U(w,t)) dw \\ + \lambda \int_0^t \int_\Omega \frac{\partial f(t,\tau)}{\partial t} p(x,y) Z(\tau,w,U(w,\tau)) dw d\tau.\end{gathered} \tag{2}$$

The integro-differential Equation (Io-DE) (2) is equivalent to IE (1). Therefore, the two equations have the same solution after neglecting the constant term.

In this article, the author is interested in studying the effect of time on the integral equation, so that the position part is linked to boundary conditions, while the time part is linked to an initial condition. There is little research that has linked position and time in integral equations. Therefore, the interest in this research is to study a nonlinear integral equation linked between position and time. In addition, this work examines and establishes the existence of a solitary solution for NIE (1), subject to specific circumstances. Furthermore, the analysis includes the examination of convergence and the assessment of error stability. A numerical technique was applied to derive a set of location-wise Hammerstein integral equations (SHIEs). In addition, the degenerate kernel method is employed to calculate the numerical solution of the SHIEs, resulting in a nonlinear algebraic system (NAS) of equations. A unique solution is obtained. Ultimately, a multitude of situations with varying kernels was resolved.

2. The Existence Solution of the NV-HIE

A fixed-point theorem and the successive approximations approach will be used to prove the existence of a single solution to Equation (1) and then converge this solution as well as the error. Therefore, we represent it in the structure of an integral operator,

$$\overline{W}U(u,t) = \frac{1}{\mu} H(u,t) + \frac{1}{\mu} WU(u,t), (\mu \neq 0) \tag{3}$$

$$WU(u,t) = \lambda \int_0^t \int_\Omega f(t,\tau) p(u,w) Z(\tau,w,U(w,\tau)) dw d\tau. \tag{4}$$

Then, assume the assumptions:

(i) Position kernel $p(u,w), u = \overline{u}(u_1,u_2,...,u_n), w = \overline{w}(w_1,w_2,...,w_n)$, check the offline condition, $\left\{ \int_\Omega \int_\Omega |p(u,w)|^2 du dw \right\}^{\frac{1}{2}} = M$, (M-constant).

(ii) Time kernel $f(t,\tau) \in C[0,T]$ check status $|f(t,\tau)| \leq \overline{f}$, ($\overline{f}$—constant).
(iii) The given function $H(u,t)$ belongs to $L_2(\Omega) \times C[0,T]$—space, and its norm is

$$\|H(u,t)\|_{L_2(\Omega)\times C[0,T]} = \max_{0\leq t\leq T}\left|\int_0^t \left\{\int_\Omega H^2(u,\tau)du\right\}^{\frac{1}{2}} d\tau\right| = G, (G-\text{constant})$$

(iv) The function $Z(t,u,U(u,t))$, for the constants $Q > L$, $Q > Q_1$, satisfies the following conditions:

$$(a)\max_{0\leq t\leq T}\left|\int_0^t \left\{\int_\Omega |Z(\tau,u,U(u,\tau))|^2 du\right\}^{\frac{1}{2}} d\tau\right| \leq Q_1\|U(u,t)\|_{L_2(\Omega)\times C[0,T]}, \|U(u,t)\| = \max_{0\leq t\leq T}\left|\int_0^t \left\{\int_\Omega |U(u,\tau)|^2 du\right\}^{\frac{1}{2}} d\tau\right|.$$

$$(b)|Z(t,u,U_1(u,t)) - Z(t,u,U_2(u,t))| \leq N(t,u)|U_1(u,t) - U_2(u,t)|,$$
$$\|N(t,u)\|_{L_2(\Omega)\times C[0,T]} = \max_{0\leq t\leq T}\left|\int_0^t \left\{\int_\Omega N^2(\tau,u)du\right\}^{\frac{1}{2}} d\tau\right| = L, (\text{L}-\text{constant}).$$

Theorem 1. *If the assumptions (i)–(iv) are verified, then Equation (1) has a single solution in* $L_2(\Omega) \times C[0,T]$, *under the condition*

$$|\mu| > |\lambda|\overline{f}MQT \tag{5}$$

In order to establish the validity of this theorem, it is necessary to examine the following lemmas:

Lemma 1. *By the assumptions (i)–(iv-a),* $\overline{W}$ *transforms* $L_2(\Omega) \times C[0,T]$ *into itself.*

Proof. Based on Equations (3) and (4), we obtain

$$\|\overline{W}U(u,t)\| \leq \frac{1}{|\mu|}\|H(u,t)\| + \frac{|\lambda|}{|\mu|}\left\|\int_0^t \int_\Omega |f(t,\tau)||P(u,w)||Z(\tau,w,U(w,\tau))|dwd\tau\right\|.$$

By utilizing the assumptions (ii)–(iii) and subsequently applying the Cauchy Schwarz inequality, we obtain,

$$\|\overline{W}U(u,t)\| \leq \frac{G}{|\mu|} + \frac{|\lambda|}{|\mu|}\overline{f}\left\|(\underbrace{\max}_{0\leq t\leq T}\int_0^t dt\,)\left\{\int_\Omega\int_\Omega |p(u,w)|^2 dudw\right\}^{\frac{1}{2}}.\max_{0\leq t\leq T}\left|\int_0^t \left\{\int_\Omega |Z(\tau,w,U(w,\tau)|^2 dw\right\}^{\frac{1}{2}} d\tau\right|\right\|.$$

Considering the given constraints (i), (iv-a), we have,

$$\|\overline{W}U(u,t)\| \leq \frac{G}{|\mu|} + \sigma\|U(u,t)\|, (\sigma = \left|\frac{\lambda}{\mu}\right|\overline{f}MQT). \tag{6}$$

Hence, $\overline{W}$ maps the ball S_ρ into itself where

$$\rho = \frac{G}{\left[|\mu| - |\lambda|\overline{f}MQT\right]}.$$

the positive values of ρ, G, lead to $\left[|\mu| - |\lambda|\overline{f}MQT\right] > 0$. This leads us to say that $\sigma < 1$.
Furthermore, W is bounded where

$$\|WU(u,t)\| \leq \sigma\|U(u,t)\|. \tag{7}$$

□

Lemma 2. *Under (i), (ii), and (iv-b), $\overline{W}$ is contraction operator in $L_2(\Omega) \times C[0,T]$.*

Proof. Regarding the two functions $\{U_1(u,t), U_2(u,t)\} \subset L_2(\Omega) \times C[0,T]$, then from Equations (3) and (4), we find

$$\begin{aligned} \|\overline{W}(U_1(u,t) &- U_2(x,t))\| \\ &\leq \frac{|\lambda|}{|\mu|}\left\|\int_0^t \int_\Omega |f(t,\tau)||p(u,w)||Z(\tau,w,U_1(w,\tau)) - Z(\tau,w,U_2(w,\tau))|dwd\tau\right\|. \end{aligned}$$

With the aid of (i), (ii), and (iv-b), and Cauchy–Schwarz inequality, we obtain

$$\left\|\overline{W}(U_1(u,t) - U_2(u,t))\right\| \leq \sigma\|U_1(u,t) - U_2(u,t)\|. \tag{8}$$

Hence, $\overline{W}$ is continuous in $L_2(\Omega) \times C[0,T]$. Moreover, under the condition $\sigma < 1$, $\overline{W}$ is a contraction operator. Hence, $\overline{W}$ has a single fixed point, which is the unique solution of Equation (1). □

3. Results the Convergence and the Error Stability of Solution

The successive approximation method was used to prove the convergence and error stability of the solution. For this, we assume $U_n(u,t) \subset U_i(u,t)_{\}}^{i=0}$, to have

$$\begin{aligned} \mu U_n(u,t) &= H(u,t) \\ &+\lambda\int_0^t \int_\Omega f(t,\tau)p(u,w)Z(\tau,w,U_{n-1}(w,\tau))dwd\tau, (n \geq 1, U_0(u,t) = H(u,t)) \end{aligned} \tag{9}$$

set,

$$\Psi_n(u,t) = U_n(u,t) - U_{n-1}(u,t) \tag{10}$$

to have

$$U_n(u,t) = \textstyle\sum_{i=1}^n \Psi_i(u,t), \Psi_0(u,t) = H(x,t). \tag{11}$$

Equation (1), yields

$$\begin{aligned} |\mu|\|U_n(u,t) - U_{n-1}(u,t)\| &\\ \leq |\lambda|\| \int_0^t \int_\Omega &|f(t,\tau)||p(u,w)|||Z(\tau,w,U_{n-1}(w,\tau)) \\ -Z(\tau,w,U_{n-2}(w,\tau))|dwd\tau\ &\|. \end{aligned}$$

Using assumptions (ii)–(iv-a), to have

$$|\mu|\|U_n(u,t) - U_{n-1}(u,t)\| \leq |\lambda|\overline{f}\left\|\int_0^t \int_\Omega |p(u,w)|N(\tau,w)|U_{n-1}(w,\tau) - U_{n-2}(w,\tau))|dwd\tau\right\|.$$

By utilizing the Cauchy–Schwarz inequality on the Hammerstein integral term, and considering the assumptions (i) and (iv-b), the inequality is simplified to

$$\|\Psi_n(u,t)\| \leq \sigma\|\Psi_{n-1}(u,t)\|, (n \geq 1). \tag{12}$$

When $n = 1$, the inequality (12), with condition (ii) takes the form

$$\|\Psi_1(u,t)\| \leq \sigma G. \tag{13}$$

By induction, we write

$$\|\Psi_n(u,t)\| \leq \sigma^n G, n = 0, 1, ..., \tag{14}$$

Since Equation (14), for $n = 0, 1, ...$, is obviously true then the sequence $\{U_n(u,t)\}$ converges, and

$$U(u,t) = \textstyle\sum_{i=0}^\infty \Psi_i(u,t). \tag{15}$$

The series (15) exhibits uniform convergence due to the uniform behavior of its terms. $\Psi_i(u,t)$ are dominated by σ^i.

To discuss the error stability, we assume $U_n(u,t)$ is the numerical solution of Equation (1); hence, we have

$$\begin{aligned}\mu R(u,t) = \{H(u,t) - H_n(u,t)\} \\ +\lambda \int_0^t \int_\Omega f(t,\tau)p(u,w)[Z(\tau,w,U(w,\tau)) - Z_n(\tau,w,U_n(w,\tau)]dwd\tau\end{aligned} \tag{16}$$

Following the same previous way, we have

$$\|R(u,t)\| \leq \frac{\|H(u,t) - H_n(u,t)\|}{|\mu| - |\lambda|\overline{f}MQT}. \tag{17}$$

The inequality (17) proved that the error is stable and has a unique representation under the condition,

$$|\mu| > |\lambda|\overline{f}MQT.$$

4. System of Hammerstein Integral Equations (SHIEs) in Position

In this part, Equation (1) employs a numerical approach to derive SHIEs in position. In order to achieve this objective, we divide $[0,T]$ as $t = t_k$,$k = 0,1,2,...,N$, then from Equation (1), we have (see [2,20])

$$\begin{aligned}\int_0^{t_k}\int_\Omega f(t_k,\tau)p(x,y)Z(\tau,w,U(w,\tau))dwd\tau \\ = \sum_{j=0}^{k} \Omega_j f(t_k,t_j)\int_\Omega p(u,w)Z(t_j,w,U(w,t_j))dw + O(\hbar_k^{p+1}), P > 0, \\ \hbar_k = \max_{0\leq j\leq k} h_j, h_j = t_{j+1} - t_j, \omega_k = \frac{1}{2}h_k, \omega_j = h_j, (j = 0,k).\end{aligned} \tag{18}$$

Using Equation (18) in Equation (1), and neglecting $O(\hbar_k^{p+1})$, we have

$$\mu U_k(u) = H_k(u) + \lambda\sum_{j=0}^{k}\omega_j f_{j,k}\int_\Omega p(u,w)Z_j(w,U_j(w))dw. \tag{19}$$

Here, we used the notations,

$$U(u,t_k) = U_k(u), H(u,t_k) = H_k(u), f(t_k,t_j) = f_{j,k}, Z(t_j,u,U(u,t_j)) = Z_j(u,U_j(u))$$

Equation (19) represents a set of n-dimensional HIEs, and its solution relies on the specified function $H_k(u), k = 0,1,...,N$, the kernel p (u, w), and the known function $Z_j(u,U_j(u))$.

5. Special Cases

(i) As an important special case let, in (19), $k = 0$ to have

$$\mu U_0(u) = H_0(u) + \lambda\omega_0 f_{0,0}\int_\Omega p(u,w)Z_0(w,U_0(w))dw. \tag{20}$$

Equation (20) represents an integral equation of Hammerstein type and its solution depends on the kind of kernel.

(ii) Let $u = \overline{u}(u_1), w = \overline{w}(w_1), Z_0(w,U_0(w)) = U_0(w), \Omega = (-1,1)$, tohave

$$\mu U_0(u) = H_0(u) + \zeta\int_{-1}^{1} p(u,w)U_0(w)dw, \zeta = \lambda\omega_0 f_{0,0} \tag{21}$$

Formula (21) represents a Fredholm integral equation of the second kind. The importance of the kernel when it takes different cases of a singular term like logarithmic kernel, Carleman kernel, Cauchy kernel, and strong singular kernel,

As an important special case when in (21) $p(u,w) = ln|u-v|$ (logarithmic kernel) hence, we have

$$\mu U_0(u) = H_0(u) + \zeta \int_{-1}^{1} ln|u-v| U_0(w) dw.$$

Differentiating the above equation with respect to u, we obtain

$$\mu \frac{dU_0(u)}{du} = \frac{dH_0(u)}{du} + \zeta \int_{-1}^{1} \frac{1}{u-v} U_0(w) dw$$

Using the substation $u = 2x-1, v = 2y-1$, we have

$$\frac{d\theta(x)}{dx} = g(x) + \overline{\zeta} \int_0^1 \frac{1}{u-v} U_0(w) dw, \left\{ g(x) = \frac{dH_0(2x-1)}{2\mu dx}, \overline{\zeta} = \frac{\zeta}{\mu} \right\} \tag{22}$$

The integral Equation (22) has appeared in both combined infrared gaseous radiation and molecular conduction, see [20].

(iii) Three-dimensional integral equation

Let $u = \overline{u}(u_1, u_2, \mathrm{u}_3), w = \overline{w}(w_1, w_2, w_3), Z_0(w, U_0(w)) = U_0(w)$, we have

$$\mu U_0(u,w) = H_0(u,w) + \beta \int_\Omega p(u-\zeta, w-\eta) U_0(\zeta,\eta) d\zeta d\eta, \beta = \lambda \omega_0 f_{0,0} \tag{23}$$

here $\Omega\ \Omega = \left\{ (\mathrm{u}, \mathrm{w}, \mathrm{v}) \epsilon \Omega : \sqrt[2]{\mathrm{u}^2 + \mathrm{w}^3} \leq \mathrm{a}, \mathrm{v} = 0 \right.$.

If $p(u-\zeta, w-\eta) = \left[(u-\zeta)^2 + (w+\eta)^2 \right]^v, 0 \leq \nu < 1$, the integral Equation (22) was nvestigated from the semi-symmetric Hertz problem for two different elastic materials in three dimensions when the modules of elasticity change according to the power law $\sigma_i = K_0 \varepsilon_i^\nu$ $(0 \leq \nu \leq 1)$,where σ_i and ε_i, $i = 1,2,3$ are the stress and strain rate intensities, respectively, while K_0, ν are physical constants.

6. The Degenerate Kernel Method and the Nonlinear Algebraic System

The straightforwardness of utilizing the Degenerate method to solve the nonlinear algebraic integral system (19) compels one to contemplate substituting the provided kernel $p(u,w)$ approximately by a kernel $p_n(u,w)$; that is

$$p_n(u,w) = \sum_{i=1}^{n} B_i(u) C_i(w). \tag{24}$$

The set of functions {Bi(u)} and {Ci(w)} are linearly independent, such that

$$\left\{ \int_\Omega \int_\Omega |p(u,w) - p_n(u,w)|^2 du dw \right\}^{\frac{1}{2}} \to 0 \ as \ n \to \infty \tag{25}$$

hence, the solution of Equation (19) associated to the kernel $p_n(u,w)$ takes the form

$$\mu U_{n,k}(u) = H_k(u) + \lambda \sum_{j=0}^{k} \omega_j f_{j,k} \int_\Omega p_n(u,w) Z_j(w, U_{n,j}(w)) dw. \tag{26}$$

Using Equation (20) in Equation (22), we have

$$\mu U_{n.k}(u) = H_k(u) + \lambda \sum_{i=1}^{n} \sum_{j=0}^{k} \omega_j f_{(j,k)} A_{i,j} B_i(u), (\mu \neq 0), k = 0,1,2,...,N. \tag{27}$$

where

$$A_{i,j} = \int_\Omega C_i(w) Z_j(w, U_{n,j}(w)) dw, j = 0,1,2,...,k$$

here, $A_{i,j}$'s are constants to be determined from the following formula

$$A_{m,j} = \int_{\Omega} C_m(w) Z_j(w, \frac{1}{\mu} H_j(w) + \frac{\lambda}{\mu} \sum_{i=1}^{n} \sum_{r=0}^{j} \omega_r f_{r,j} A_{i,j} B_i(w)) dw, (m = 1, 2, ..., n).$$

Define

$$E_{m,j}(A_{1,j}, A_{2,j}, ..., A_{n,j}) = \int_{\Omega} C_m(w) Z_j(w, \frac{1}{\mu} H_j(w) + \frac{\lambda}{\mu} \sum_{i=1}^{n} \sum_{r=0}^{j} \omega_r f_{r,j} A_{i,j} B_i(w)) dw, \tag{28}$$

Equation (28) represents a system of NAEs that can be written as a matrix equation

$$\begin{bmatrix} A_{1,j} \\ A_{2,j} \\ A_{3,j} \\ . \\ . \\ . \\ A_{n,j} \end{bmatrix} = \begin{bmatrix} E_{1,j}(A_{1,j}, A_{2,j}, ..., A_{n,j}) \\ E_{2,j}(A_{1,j}, A_{2,j}, ..., A_{n,j}) \\ E_{3,j}(A_{1,j}, A_{2,j}, ..., A_{n,j}) \\ . \\ . \\ . \\ E_{n,j}(A_{1,j}, A_{2,j}, ..., A_{n,j}) \end{bmatrix}, \tag{29}$$

the nonlinear algebraic system (29) can be solved numerically.

The Existence of a Single Solution of the Nonlinear Algebraic System

This section will provide an exposition on the existence and validation of a distinct NAS solution (24). To accomplish this, the following theorem will be formulated.

Theorem 2. *Assume that the known continuous functions $Z_j(w, \psi(w, A_{i,j}))$ in Equation (27) satisfy the following conditions,*

$$\left\{ \int_{\Omega} \left| Z_j(w, \psi(w, A_{i,j})) \right|^2 dw \right\}^{\frac{1}{2}} \leq L \left(\sum_{i=1}^{n} |A_{i,j}|^2 \right)^{\frac{1}{2}}, (L \text{ is constant }) \tag{30}$$

and,

$$\left| Z_j(w, \psi(w, A_{i,j})) - Z_j(w, \psi(w, D_{i,j})) \right| \leq M_1 \left| \psi(w, A_{i,j}) - \psi(w, D_{i,j}) \right|, (M_1 \text{is constant}) \tag{31}$$

then, the NAS (29) has a single solution $\overline{A}_j$, and $U_{n,k}(u)$ is the single solution of Equation (27) in ℓ_2-space.

To demonstrate the validity of this theorem, it is necessary to examine the following two lemmas.

Lemma 3. *By the aid of the condition (30), the operator $\overline{E}_j$ of Equation (28) maps ℓ_2-space into itself.*

Proof. Let V be the set of functions $\Xi = \{\xi_i\}$ in ℓ_2 such that

$$\|\Xi\|_{\ell_2} = \left(\sum_{i=1}^{\infty} |\xi_i|^2 \right)^{\frac{1}{2}} \leq \beta, (\beta - \text{constant}).$$

From Equation (27), we have

$$\left| E_{m,j}(A_{1,j}, A_{2,j}, ..., A_{n,j}) \right| \leq \int_{\Omega} |C_m(w)| \left| w, \frac{1}{\mu} H_j(w) + \frac{\lambda}{\mu} \sum_{i=1}^{n} \sum_{r=0}^{j} \omega_r f_{r,j} A_{i,j} B_i(w))) \right| dw.$$

Hence, after applying Cauchy–Schwarz inequality, and using condition (30), we have

$$\left(\sum_{m=1}^{n}\left|E_{m,j}(A_{1,j},A_{2,j},...,A_{n,j})\right|^2\right)^{\frac{1}{2}} \leq M_2\left(\sum_{i=1}^{n}|A_{i,j}|^2\right)^{\frac{1}{2}}, (M_2 L\left(\sum_{m=1}^{n}\int_{\Omega}|C_m(w)|^2 dw\right)^{\frac{1}{2}})\text{constant}),$$

as $n \to \infty$, the last inequality yields

$$\left\|\overline{E}_j(\overline{A}_j)\right\|_{\ell_2} \leq M_2\left\|\overline{A}_j\right\|_{\ell_2}. \tag{32}$$

Hence, $\overline{H}_i$ is a bounded operator that maps the set U into itself, where

$$\beta = M_2\left\|\overline{A}^{(j)}\right\|_{\ell_2}.$$

□

Lemma 4. *Under the condition (31), $\overline{E}_j$ is a contraction mapping in ℓ_2.*

For the functions $\overline{A}_j = (A_{1,j}, A_{2,j}, ..., A_{n,j})$ and $\overline{D}_j = (D_{1,j}, D_{2,j}, ..., D_{n,j})$ in ℓ_2, Equation (24) leads to

$$\begin{gathered}\left|E_{m,j}(A_{1,j},A_{2,j},...,A_{n,j}) - E_{m,j}(D_{1,j},D_{2,j},...,D_{n,j})\right| \leq \\ \int_{\Omega}|C_m(w)||Z_j(w,\tfrac{1}{\mu}H_j(w) + \tfrac{\lambda}{\mu}\sum_{i=1}^{n}\sum_{r=0}^{j}\omega_r f_{r,j}A_{i,j}B_i(w)) - Z_j(w,\tfrac{1}{\mu}H_j(w) \\ +\tfrac{\lambda}{\mu}\sum_{i=1}^{n}\sum_{r=0}^{j}\omega_r f_{r,j}D_{i,j}B_i(w))|dw.\end{gathered}$$

Introducing condition (31), then applying Cauchy–Schwarz inequality three times, the above inequality takes the form

$$\left(\sum_{m=1}^{n}\left|H_{m,j}(A_{1,j},A_{2,j},...,A_{n,j}) - H_{m,j}(D_{1,j},D_{2,j},...,D_{n,j})\right|^2\right)^{\frac{1}{2}} \leq M_3\left(\sum_{i=1}^{n}|A_{i,j}-D_{i,j}|^2\right)^{\frac{1}{2}},$$

$$M_3 = \frac{|\lambda|}{|\mu|}M_1\left(\sum_{r=0}^{j}\left|u^{(r)}\right|^2\right)^{\frac{1}{2}}\left(\sum_{r=0}^{j}\left|F^{(r,j)}\right|^2\right)^{\frac{1}{2}}\left(\sum_{m=1}^{n}\int_{\Omega}|C_m(y)|^2dy\right)^{\frac{1}{2}}\left(\sum_{i=1}^{n}\int_{\Omega}|B_i(y)|^2dy\right)^{\frac{1}{2}}.$$

As $n \to \infty$, the previous inequality can be reduced to

$$\left\|\overline{E}_j(\overline{A}_j) - \overline{E}_j(\overline{D}_j)\right\|_{\ell_2} \leq M_3\left\|\overline{A}_j - \overline{D}_j\right\|_{\ell_2}. \tag{33}$$

Thus, $\overline{E}_j$ is a continuous operator in the space ℓ_2. If $M_3 < 1$, then $\overline{E}_j$ is a contraction operator. Hence, $\overline{E}_j$ has a unique fixed point $\overline{A}_j$, which is the unique solution of the algebraic system (27). In view of Theorem 2, the algebraic system (27) has a single solution $U_{n,k}(u)$ in ℓ_2.

7. Examples and Numerical Results

Example 1. *For the NV-HIE*

$$U(u,t) - \int_0^t\int_0^1 \tau^3(1+uw)U^{\ell}(w,\tau)dwd\tau = H(u,t), \ell = 1,2,...,N, (U(u,t) = ut). \tag{34}$$

If we divide the interval [0, T] as $0 = t_0 < t_1 < t_2 < t_3 = t, t = t_k; k = 0,1,2,3$, and using the degenerate method, we obtain

$$U_k(u) - \sum_{j=0}^{k}\sum_{m=0}^{n}\omega_j t_j^3\frac{u^m}{m!}A_{j,m} = H_k(u), (k = 0,1,2,3), \tag{35}$$

where

$$A_{k,m} = \int_0^1 y^m \left[H_k(w) + \sum_{j=0}^{k} \sum_{m=0}^{n} \omega_j t_j^3 \frac{u^m}{m!} A_{j,m} \right]^2 dw, H_k(u) = H(u, t_k).$$

The solution of Equation (35) gives the following results,

$$U_0(u) = 0, U_1(u) = \frac{ut}{3}, U_2(u) = \frac{2ut}{3}, U_3(u) = ut.$$

Here, $U_3(u)$ is the exact solution of Equation (34).

Example 2. *For the NV-HIE*

$$U(u,t) - \int_0^t \int_0^1 \tau^3 e^{uw} U^\ell(w,\tau) dw d\tau = H(u,t), \ell = 1, 2, ..., N, (U(u,t) = ut). \tag{36}$$

Approximate the kernel of Equation (36) $p(u,w) = e^{uw}$ in the form,

$$p(u,w) \simeq p_n(u,w) = \sum_{m=0}^{n} \frac{(uw)^m}{m!}, \tag{37}$$

where

$$\left\{ \int_0^1 \int_0^1 |p(u,w) - p_n(u,w)|^2 du dw \right\}^{\frac{1}{2}} \to 0 \text{ as } n \to \infty.$$

Using the degenerate kernel, we obtain

$$\begin{aligned} U_k(u) - \sum_{j=0}^{k} \sum_{m=0}^{n} \omega_j t_j^3 \tfrac{u^m}{m!} A_{j,m} = H_k(u), A_{k,m} \\ = \int_0^1 w^m \left[H_k(w) + \sum_{j=0}^{k} \sum_{m=0}^{n} \omega_j t_j^3 \tfrac{u^m}{m!} A_j^{(m)} \right]^2 dw, (k = 0, 1, 2, 3). \end{aligned} \tag{38}$$

The solution of Equation (38), gives $U_0(u) = 0, U_1(u) = \frac{ut}{3}, U_2(u) = \frac{2ut}{3}, U_3(u) = ut$. Here, $U_3(u)$ is the exact solution of Equation (36).

Example 3. *Assume the kernel in the Legendre or Chebyshev polynomials forms. Then, we have two cases as follows,*

Example 3.1. *Consider the **MIE** with the kernel in Legendre polynomial form,*

$$U(u,t) = H(x,t) + \int_0^t \int_{-1}^1 \tau^2 \sum_{n=0}^{20} P_n(u) P_n(w) U^\ell(w,\tau) dw d\tau;$$

The exact solution is $U(u,t) = u^2 + t^2$.

In the third example, the kernel generation method was applied when the kernel is in the form of a Legendre polynomial, considering the difference in time. The equation was also applied when it was linear and when it was nonlinear. From Tables 1–3, it was noted that the error in the linear case is slightly higher than the error in the nonlinear case. Also, as time increases, the cumulative error increases.

Table 1. Discusses the numerical results and estimating errors at $\mu = 1, \lambda = 1, T = 0.01$, in the linear case $l = 1$, and nonlinear case.

u	$Exact$	U_{linear}	$U_{nonlinear}$	$Eerror_{linear}$	$Error_{nonlinear}$
-1	1.0001	1.000027301	1.000156796	7.2699×10^{-5}	5.6796×10^{-5}
-0.5	0.2501	0.250558794	0.2501511588	4.58794×10^{-4}	5.511588×10^{-5}
0	0.0001	0.00032278	0.000093462	2.2278×10^{-4}	6.538×10^{-6}
0.5	0.2501	0.25060319	0.2503023022	5.0319×10^{-4}	2.023022×10^{-4}
1	1.0001	1.00027034	1.0000273	1.7034×10^{-4}	7.27×10^{-5}

Table 2. Discusses the numerical results and estimating errors at $\mu = 1, \lambda = 1, T = 0.4$, in the linear case $l = 1$, and nonlinear case.

u	$Exact$	U_{linear}	$U_{nonlinear}$	$Eerror_{linear}$	$Error_{nonlinear}$
-1	1.16	1.209464729	1.160215981	0.04946429	2.15981×10^{-4}
-0.5	0.41	0.4419580477	0.4099824773	0.0319580477	1.75227×10^{-5}
0	0.16	0.1553572123	0.1599678394	4.6427877×10^{-3}	3.21606×10^{-5}
0.5	0.41	0.3977882159	0.4099281713	0.0122117841	7.18287×10^{-5}
1	1.16	1.209464729	1.160085598	00.049464729	8.5598×10^{-5}

Table 3. Discusses the numerical results and estimating errors at $\mu = 1, \lambda = 1, T = 0.8$, in the linear case $l = 1$, and nonlinear case.

u	$Exact$	U_{linear}	$U_{nonlinear}$	$Eerror_{linear}$	$Error_{nonlinear}$
-1	1.64	1.8510286885	1.640901375	0.211028688	5.4191×10^{-4}
-0.5	0.89	0.8371583441	0.8896882523	0.0528416559	3.117477×10^{-4}
0	0.64	0.6104412354	0.6396523326	0.0295587646	3.476674×10^{-4}
0.5	0.89	0.839453621	0.8896515856	0.050546379	3.484144×10^{-4}
1	1.64	1.851028686	1.640038297	0.211028686	3.8297×10^{-5}

Example 3.2. *Consider the MIE with the kernel in the Chebyshev polynomial form,*

$$U(u,t) = H(u,t) + \int_0^t \int_{-1}^1 \tau^2 \sum_{n=0}^{20} T_n(u) T_n(w) U^l(w,\tau) dw d\tau;$$

The exact solution is $U(u,t) = u^2 + t^2$.

In this example, the kernel generation method was also applied in the linear and nonlinear integral equation at different times for the continuous time kernel. The position kernel was also imposed in the form of a Chebyshev polynomial function of the first kind. The resulting error was also studied at different times, and this is clear in Tables 4–6.

Table 4. Discusses the numerical results and estimating errors at $\mu = 1, \lambda = 1, T = 0.01$, in the linear case $l = 1$, and nonlinear case.

u	$Exact$	U_{linear}	$U_{nonlinear}$	$Eerror_{linear}$	$Error_{nonlinear}$
-1	1.0001	1.000645552	1.000156796	5.45552×10^{-4}	5.6796×10^{-4}
-0.5	0.2501	0.2499299037	0.2508547062	7.547062×10^{-4}	1.700963×10^{-4}
0	0.0001	0.0006081	0.0001345009	5.081×10^{-4}	3.45009×10^{-4}
0.5	0.2501	0.249258	0.2498976982	8.42×10^{-4}	2.23018×10^{-4}
1	1.0001	1.000645552	1.0002703450	5.45552×10^{-4}	1.70345×10^{-4}

Table 5. Discusses the numerical results and estimating errors at $\mu = 1, \lambda = 1, T = 0.4$ in the linear case $l = 1$, and nonlinear case.

u	$Exact$	U_{linear}	$U_{nonlinear}$	$Eerror_{linear}$	$Error_{nonlinear}$
-1	1.16	1.109657913	1.159812825	0.050342087	1.87175×10^{-4}
-0.5	0.41	0.394436943	0.4101825043	0.015563057	1.825043×10^{-4}
0	0.16	0.1509816382	0.1601612092	9.0183618×10^{-3}	1.612092×10^{-4}
0.5	0.41	0.4003211	0.40981749	9.6789×10^{-3}	1.8251×10^{-4}
1	1.16	1.21034208	1.160056829	0.05034208	5.6829×10^{-5}

Table 6. Discusses the numerical results and estimating errors at $\mu = 1, \lambda = 1, T = 0.8$, in the linear case $l = 1$, and nonlinear case.

u	$Exact$	U_{linear}	$U_{nonlinear}$	$Eerror_{linear}$	$Error_{nonlinear}$
-1	1.64	1.85248633	1.64054191	0.21248633	5.4191×10^{-4}
-0.5	0.89	0.78216442	0.890210195	0.10783558	2.10195×10^{-4}
0	0.64	0.6104412354	0.6403476674	0.0295587646	3.476674×10^{-4}
0.5	0.89	0.839453621	0.88965158	0.050546379	3.4842×10^{-4}
1	1.64	1.851028686	1.640038297	0.211028686	3.8297×10^{-5}

8. Conclusions

The study successfully proves the existence of a solitary solution for NMIE (1) under specified conditions. The research includes an analysis of convergence and an evaluation of error stability. To solve the problem, a numerical technique is utilized to transform the problem into a set of location-wise Hammerstein integral equations (SHIEs). The degenerate kernel method is a powerful technique to compute the numerical solutions of these SHIEs, leading to a nonlinear algebraic system (NAS) of equations that yields a unique solution. The study concludes by resolving numerous scenarios involving different kernels, including the kernels in the form of Legendre and Chebyshev polynomials, respectively, and calculating the numerical solution in the linear and nonlinear cases. We deduce that the error estimates associated with the nonlinear case are less than the linear ones; see Tables 1–6 and Figures 1–4.

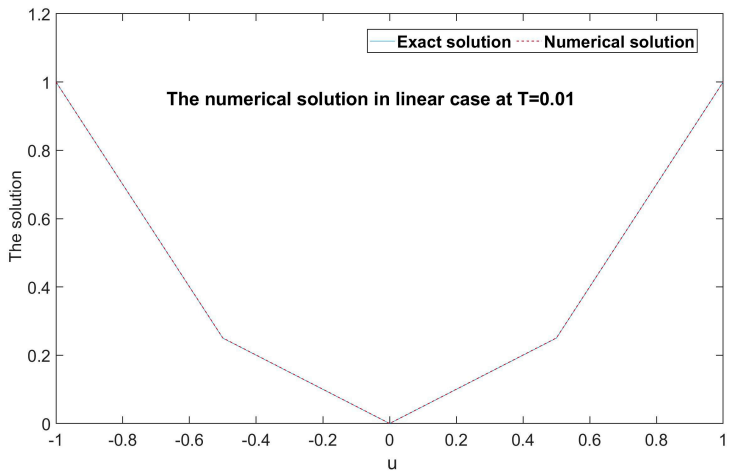

Figure 1. Comparison between the exact solution and numerical solution in the linear case of the integral equation at T = 0.01.

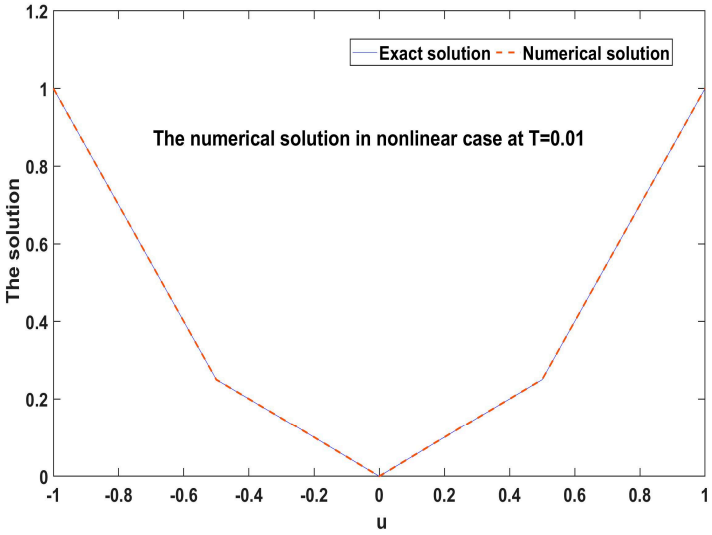

Figure 2. Comparison between the exact solution and numerical solution in the nonlinear case of the integral equation at T = 0.01.

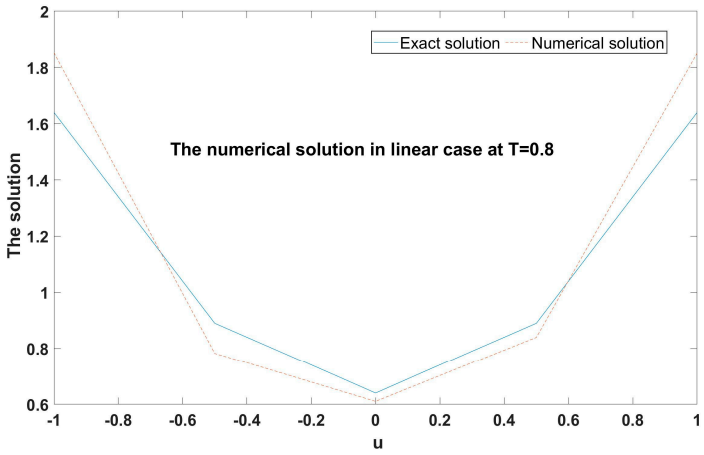

Figure 3. Comparison between the exact solution and numerical solution in the linear case of the integral equation at T = 0.8.

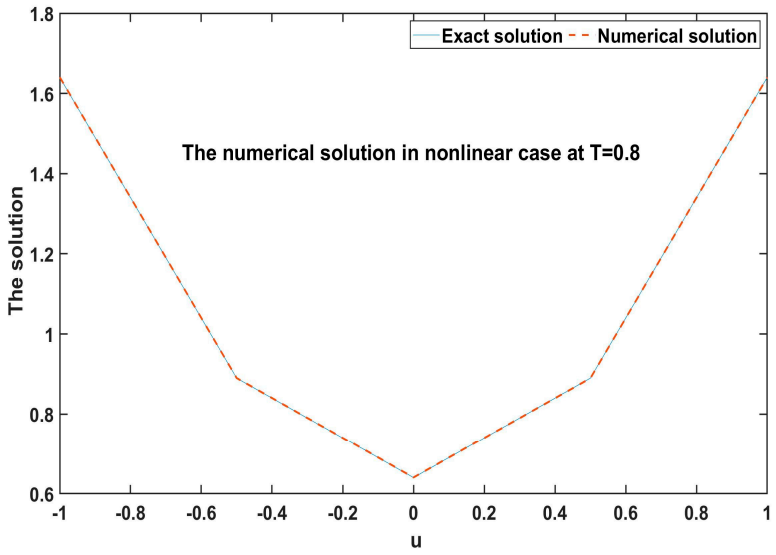

Figure 4. Comparison between the exact solution and numerical solution in the nonlinear case of the integral equation at T = 0.8.

Funding: This research received no external funding.

Data Availability Statement: Data are contained within the article.

Conflicts of Interest: The author declares no conflict of interest.

References

1. Alhazmi, S.E.A. New Model for Solving Mixed Integral Equation of the First Kind with Generalized Potential Kernel. *J. Math. Res.* **2017**, *9*, 18–29. [CrossRef]
2. Nemati, S.; Lima, P.M.; Ordokhani, Y. Numerical solution of a class of two-dimensional nonlinear Volterra integral equations using Legendre polynomials. *J. Comput. Appl. Math.* **2013**, *242*, 53–69. [CrossRef]
3. Hafez, R.M.; Youssri, Y.H. Spectral Legendre-Chebyshev treatment of 2d linear and nonlinear mixed Volterra-Fredholm integral equation. *Math. Sci. Lett.* **2020**, *9*, 37–47.
4. Abdou, M.A.; Soliman, A.; Abdel-Aty, M. Analytical results for quadratic integral equations with phase-clag term. *J. Appl. Anal. Comput.* **2020**, *10*, 1588–1598. [CrossRef] [PubMed]
5. El-Sayed, A.M.A.; Ahmed, G.R. Solvability of a coupled system of functional integro-differential equations with infinite point and Riemann-Stieltjes integral conditions. *Appl. Math. Comput.* **2020**, *370*, 124918. [CrossRef]
6. El-Sayed, A.M.A.; Ahmed, R.G. Infinite point and Riemann Stieltjes integral conditions for an integro differential equation. *Nonlinear Anal. Model. Control* **2019**, *24*, 733–754. [CrossRef]
7. Mohamed, D.S. Application of Lerch polynomials to approximate solution of singular Fredholm integral equations with Cauchy kernel. *Appl. Math. Inf. Sci.* **2022**, *16*, 565–574.
8. Cayan, S.; Sezer, M.A. Novel study based on Lerch polynomials for approximate solutions of pure neumann problem. *Int. J. Appl. Comput. Math.* **2022**, *8*, 8. [CrossRef]
9. Ali, M.R.; Mousa, M.M.; Ma, W.-X. Solution of nonlinear Volterra integral equations with weakly singular kernel by using the HOBW method. *Adv. Math. Phys.* **2019**, *2019*, 1705651. [CrossRef]
10. El-Sayed, S.M.; Abdel-Aziz, M.R. A comparison of Adomian's decomposition method and wavelet-Galerkin method for solving integro-differential equations. *Appl. Math. Comp.* **2003**, *136*, 151–159. [CrossRef]
11. Bin Jebreen, H.; Dassios, I. On the Wavelet Collocation Method for Solving Fractional Fredholm Integro-Differential Equations. *Mathematics* **2022**, *10*, 1272. [CrossRef]
12. Mahdy, A.M.S.; Abdou, M.A.; Mohamed, D.S. Computational methods for solving higher-order (1 + 1) dimensional mixed difference integro-differential equations with variable coefficients. *Mathematics* **2023**, *11*, 2045. [CrossRef]
13. Zhang, T.; Li, Y. Exponential Euler scheme of multi-delay Caputo–Fabrizio fractional-order differential equations. *Appl. Math. Lett.* **2022**, *124*, 107709. [CrossRef]
14. Abdou, M.A.; Basseem, M. Thermopotential function in position and time for a plate weakened by curvilinear hole. *Arch. Appl. Mech.* **2022**, *92*, 867–883. [CrossRef]
15. Akram, T.; Ali, Z.; Rabiei, F.; Shah, K.; Kumam, P. A Numerical Study of Nonlinear Fractional Order Partial Integro-Differential Equation with a Weakly Singular Kernel. *Fractal Fract.* **2021**, *5*, 85. [CrossRef]
16. Kuzmina, K.; Marchevsky, I. The boundary integral equation solution in vortex methods with the airfoil surface line discretization into curvilinear panels. In Proceedings of the Topical Problems of Fluid Mechanics, Prague, Czech Republic, 20–22 February 2019; pp. 131–138.
17. Lienert, M.; Tumulka, R. A new class of Volterra-type integral equations from relativistic quantum physics. *J. Integral Equ. Appl.* **2019**, *31*, 535–569. [CrossRef]
18. Gao, J.; Condon, M.; Iserles, A. Spectral computation of highly oscillatory integral equations in laser theory. *J. Comput. Phys.* **2019**, *395*, 351–381. [CrossRef]
19. Ata, K.; Sahin, M. An integral equation approach for the solution of the Stokes flow with Hermite surfaces. *Eng. Anal. Bound. Elem.* **2018**, *96*, 14–22. [CrossRef]
20. Matoog, R.T. Treatments of probability potential function for nuclear integral equation. *J. Phys. Math.* **2017**, *8*, 1000226.